Intrinsic (Gas-Phase) Binding of Co^{2+} and Ni^{2+} by Peptides: A Direct Reflection of Aqueous-Phase Chemistry

Alex Reiter, Jeanette Adams,* and Hong Zhao

Contribution from the Department of Chemistry and the Emory University Mass Spectrometry Center, Emory University, Atlanta, Georgia 30322

*Received February 9, 1994. Revised Manuscript Received May 3, 1994**

Abstract: The gas-phase binding chemistry between Ca^{2+}, Co^{2+}, and Ni^{2+} and 33 tri- through decapeptides is evaluated with respect to aqueous-phase and theoretical chemistry. Metastable ion decompositions of tetrapeptide and larger peptide complexes that contain either hydrocarbon amino acid side chains or Pro reveal the intrinsic binding preferences. Tripeptide complexes do not. Interactions with the Ca^{2+}-specific binding sequence in staphylococcal nuclease and with the Asp side chain in the third position from the N-terminus are also presented. For Co^{2+} and Ni^{2+}, aqueous-phase chemistry is reflected in the gas-phase results. Mass spectrometry detects some weakly abundant, less favorable complexes, species that aqueous-phase studies do not detect. Gas-phase complexes of Ca^{2+} are not seen in solution because aqueous equilibria favor precipitation of $Ca(OH)_2$. Solution-phase binding interactions between Co^{2+} and Ni^{2+}, however, are intrinsic, independent of solvation. Metastable ion decomposition mass spectrometry has a future in the direct elucidation of important metal ion binding sites in peptides and proteins.

Introduction

Transition metal ions such as Co^{2+} and Ni^{2+} are vital for a variety of biochemical reactions.[1] Most of Co^{2+} in humans is present in vitamin B_{12}.[1a] Several proteins such as jack bean urease, hydrogenase, methyl coenzyme M reductase, and carbonyl dehydrogenase contain functionally significant Ni^{2+}.[1b,c]

Aqueous- and solid-phase binding interactions between Ca^{2+}, Co^{2+}, and Ni^{2+} and peptides or proteins have been extensively studied.[2-14] Only a few studies of the intrinsic, or gas-phase, chemistry have been performed.[15-17] We originally investigated intrinsic binding interactions between alkaline earth metal ions and peptides by studying collision-induced decomposition (CID) of the cationic gas-phase $(M + Cat^{2+} - H)^+$ complexes.[15] More recently, we presented both experimental and theoretical evidence that specific side-chain binding interactions occur between alkaline earth metal ions and tripeptides and larger peptides in their anionic $(M + Cat^{2+} - 3H)^-$ complexes.[16a] We addressed the binding chemistry involved in losses of serine (Ser) and threonine (Thr) side chains.[16b] We showed that the chemistry of Ca^{2+}-specific binding sites in proteins is an intrinsic feature of the structures.[16c] We originally presented CID spectra of complexes between Co^{2+} and Ni^{2+} and a pentapeptide that display sharp differences in the intrinsic binding chemistry of alkaline earth metal ions vs transition metal ions.[16a] Similarly, Hu and Gross most recently published CID spectra of complexes of di- and tripeptides that contain hydrocarbon amino acids.[17c]

We now present a more detailed comparison of the gas-phase binding chemistry between Ca^{2+}, Co^{2+}, and Ni^{2+} and tri- through hexapeptides. Metastable ion decomposition spectra of peptides that contain either hydrocarbon amino acid side chains or Pro reveal the fundamental binding interactions. Special binding interactions with the Ca^{2+}-specific binding sequence -Asp-Val-Pro- and the aspartic acid (Asp) side chain are also discussed. The gas-phase binding chemistry between Co^{2+} and Ni^{2+} and peptides that contain His and other important side chains will be presented in another paper.

Results

Formation of anionic $(M + Cat^{2+} - 3H)^-$ complexes between peptides and divalent metal ions requires deprotonation of three

* Abstract published in *Advance ACS Abstracts*, July 15, 1994.

(1) (a) Kendrick, M. J.; May, M. T.; Plishka, M. J.; Robinson, K. D. *Metals in Biological Systems*; Ellis Horwood: Chichester, England, 1992; pp 70–79. (b) Kendrick, M. J.; May, M. T.; Plishka, M. J.; Robinson, K. D. *Metals in Biological Systems*; Ellis Horwood: Chichester, England, 1992; pp 150–156. (c) Sigel, H. In *Metal Ions in Biological Systems*; Sigel, H., Ed.; Marcel Dekker: New York, 1988; Vol. 23.

(2) Sóvágó, I. In *Biocoordination Chemistry*; Burger, K., Ed.; Ellis Horwood: Chichester, England, 1990; pp 135–184.

(3) (a) Martin, R. B.; Chamberlin, M.; Edsall, J. T. *J. Am. Chem. Soc.* **1960**, *82*, 495–498. (b) Dorigatti, T. F.; Billo, E. J. *J. Inorg. Nucl. Chem.* **1975**, *37*, 1515–1520. (c) Freeman, H. C.; Guss, J. M.; Sinclair, R. L. *Acta. Crystallogr.* **1978**, *B34*, 2459–2466. (d) Formicka-Kozlowska, G.; Kozlowski, H.; Jezowska-Trzebiatowska, B. *Inorg. Chim. Acta* **1977**, *25*, 1–5. (e) Sigel, H.; Martin, R. B. *Chem. Rev.* **1982**, *82*, 385–426. (f) Pettit, L. D.; Pyburn, S.; Kozlowski, H.; Reverend, B. D.; Liman, F. *J. Chem. Soc., Dalton Trans.* **1989**, 1471–1475.

(4) Siemion, I. Z.; Kubik, A.; Jezowska-Bojczuk, M.; Kozyloski, H. *J. Inorg. Chem.* **1984** *22*, 137–141.

(5) Formicka-Kozlowska, G.; Kozlowski, H.; Bezer, M.; Pettit, L. D.; Kupryszewski, G.; Przybylski, J. *Inorg. Chim. Acta* **1981**, *56*, 79–82.

(6) Bezer, M.; Pettit, L. D.; Steel, I.; Bataille, M.; Djemil, S.; Kozlowski, H. *J. Inorg. Biochem.* **1984**, *20*, 13–21.

(7) (a) Bataille, M.; Formicka-Kozlowska, G.; Kozlowski, H.; Pettit, L. D.; Steel, I. *J. Chem. Soc., Chem. Commun.* **1984**, 231–232. (b) Pettit, L. D.; Steel, I.; Formicka-Kozlowska, G.; Tatarowski, T.; Bataille, M. *J. Chem. Soc., Dalton Trans.* **1985**, 535–539. (c) Pettit, L. D.; Livera, C.; Steel, I.; Bataille, M.; Cardon, C. *Polyhedron* **1987**, *6*, 45–52.

(8) Reverend, B. D.; Andrianarijaona, L.; Livera, C.; Pettit, L. D.; Steel, I.; Kozlowski, H. *J. Chem. Soc., Dalton Trans.* **1986**, 2221–2226.

(9) (a) Reverend, B. D.; Lebkiri, A.; Livera, C.; Pettit, L. D. *Inorg. Chim. Acta* **1986**, *124*, L19–L22. (b) Sóvágó, I.; Kiss, T.; Gergely, A. *Inorg. Chim. Acta* **1984**, *93*, L53–L55. (c) Sóvágó, I.; Radomska, B.; Schön, I.; Nyéki, O. *Polyhedron* **1990**, *9*, 825–830.

(10) (a) Sakurai, T.; Nakahara, A. *Inorg. Chim. Acta* **1979**, *34*, L243–L244. (b) Sakurai, T.; Nakahara, A. *Inorg. Chem.* **1980**, *19*, 847–853. (c) Sarkar, B.; Rakhit, G. *J. Inorg. Biochem.* **1981**, *15*, 233–241.

(11) Einspahr, E.; Bugg, C. E. In *Metal Ions in Biological Systems*; Sigel, H., Ed.; Marcel Dekker: New York, 1984; Vol. 17, pp 51–97.

(12) Freeman, H. C.; Guss, J. M. *Acta. Crystallogr.* **1978**, *B34*, 2451–2458.

(13) (a) Li, N. C.; Doody, B. E.; White, J. M. *J. Am. Chem. Soc.* **1957**, *79*, 5859–5863. (b) Michailidis, M. S.; Martin, R. B. *J. Am. Chem. Soc.* **1969**, *91*, 4683–4689. (c) Morris, P. J.; Martin, R. B. *Inorg. Chem.* **1971**, *10*, 964–968. (d) Gillard, R. D.; Phipps, D. A. *J. Chem. Soc. A* **1971**, 1074–1082.

(14) (a) Van Der Helm, D.; Willoughby, T. V. *Acta. Crystallogr.* **1969**, *B25*, 2317–2326. (b) Eastman, M. A.; Pedersen, L. G.; Hiskey, R. G.; Pique, M.; Koehler, K. A.; Gottschalk, K. E.; Némethy, G.; Scheraga, H. A. *Int. J. Peptide Protein Res.* **1986**, *27*, 530–553. (c) Maynard, A. T.; Eastman, M. A.; Darden, T.; Deerfield, D. W.; Hiskey, R. G.; Pedersen, L. G. *Int. J. Peptide Protein Res.* **1988**, *31*, 137–149.

(15) Teesch, L. M.; Adams, J. *J. Am. Chem. Soc.* **1990**, *112*, 4110–4120.

(16) (a) Zhao, H.; Reiter, A.; Teesch, L. M.; Adams, J. *J. Am. Chem. Soc.* **1993**, *115*, 2854–2863. (b) Reiter, A.; Teesch, L. M.; Zhao, H.; Adams, J. *Int. J. Mass Spectrom. Ion Processes* **1993**, *127*, 17–26. (c) Reiter, A.; Zhao, H.; Adams, J. *Org. Mass Spectrom.* **1994**, *28*, 1596–1601.

(17) (a) Hu, P.; Gross, M. L. *J. Am. Chem. Soc.* **1992**, *114*, 9153–9160. (b) Hu, P.; Gross, M. L. *J. Am. Chem. Soc.* **1992**, *114*, 9161–9169. (c) Hu, P.; Gross, M. L. *J. Am. Chem. Soc.* **1993**, *115*, 8821–8828.

0002-7863/94/1516-7827$04.50/0

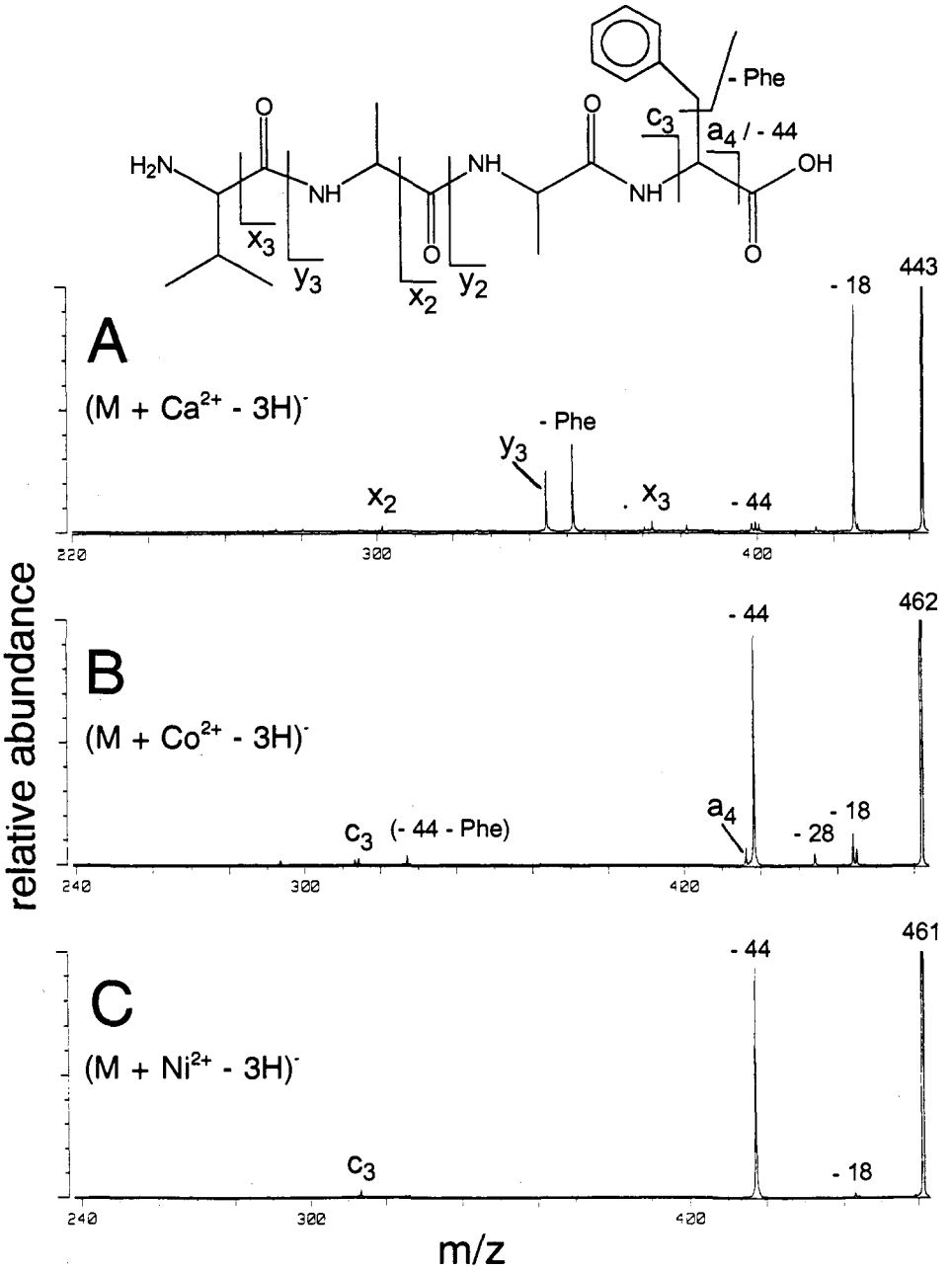

Figure 1. Metastable ion decomposition spectra of (A) $(M + Ca^{2+} - 3H)^-$, (B) $(M + Co^{2+} - 3H)^-$, and (C) $(M + Ni^{2+} - 3H)^-$ complexes of Val-Ala-Ala-Phe. Ions labeled x_{n-m} and y_{n-m} are $(x_{n-m} + Ca^{2+} - 2H)^-$ and $(y_{n-m} + Cat^{2+} - 2H)^-$ ions, respectively. Ions labeled a_4 and c_3 are $(a_4 + Co^{2+} - 4H)^-$ and $(c_3 + Cat^{2+} - 2H)^-$ ions, respectively. Loss of the Phe side chain as C_7H_8 in Figure 1A is labeled as –Phe. Ions labeled (– 44 – Phe) in Figure 1B are formed by losses of both CO_2 and the Phe side chain as $C_7H_7^{\bullet}$.

peptide functional groups. They can include the N-terminal amine, amide NH groups, the C-terminal carboxylate, and some protic amino acid side chains. The preferential formation of structurally-specific chelates causes preferential formation of structurally distinct product ions that directly reveal the metal ion binding site.[16]

Metastable ion decompositions probe low-energy reacting configurations of the precursor complexes. The most structurally revealing reactions are low-energy charge-induced cleavages that occur in immediate proximity to the metal-ion binding site. The reactions leave the binding site intact, and the product complexes contain the intact chelate structure. High-energy collisional activation instead could cause high-energy reactions that might not reflect either the intrinsic stability of the binding site or its location in the peptide chain. CID might involve cleavages of the chelate structure itself or induce charge-remote reactions[18] whose product ions would not directly reveal the precise location of the metal ion binding site.

Binding Sites in Tetrapeptides and Larger Peptides That Contain Hydrocarbon Amino Acid Side Chains. The only sites for deprotonation of peptides in $(M + Cat^{2+} - 3H)^-$ complexes that contain hydrocarbon amino acid side chains are the N-terminal amine, amide NH groups, and the C-terminal carboxylate. Alkaline earth metal ions intrinsically prefer binding either to the C-terminal carboxylate and two deprotonated amides or to three deprotonated amides in tripeptides and larger peptides that contain hydrocarbon side chains.[16] For example, $(M + Ca^{2+} - 3H)^-$ complexes of VAAF that contain the metal ion bound to three deprotonated amides give an abundant loss of H_2O (–18) (Figure 1A). Other isomers, however, give C-terminal $(y_3 + Ca^{2+} - 2H)^-$ sequence ions.[19] We showed previously[16a] that the most energetically favorable, and thus most abundant, precursors that give the $(y_3 + Ca^{2+} - 2H)^-$ ions contain Ca^{2+} bound to either

(18) Adams, J. *Mass Spectrom. Rev.* **1990**, *9*, 141–186.

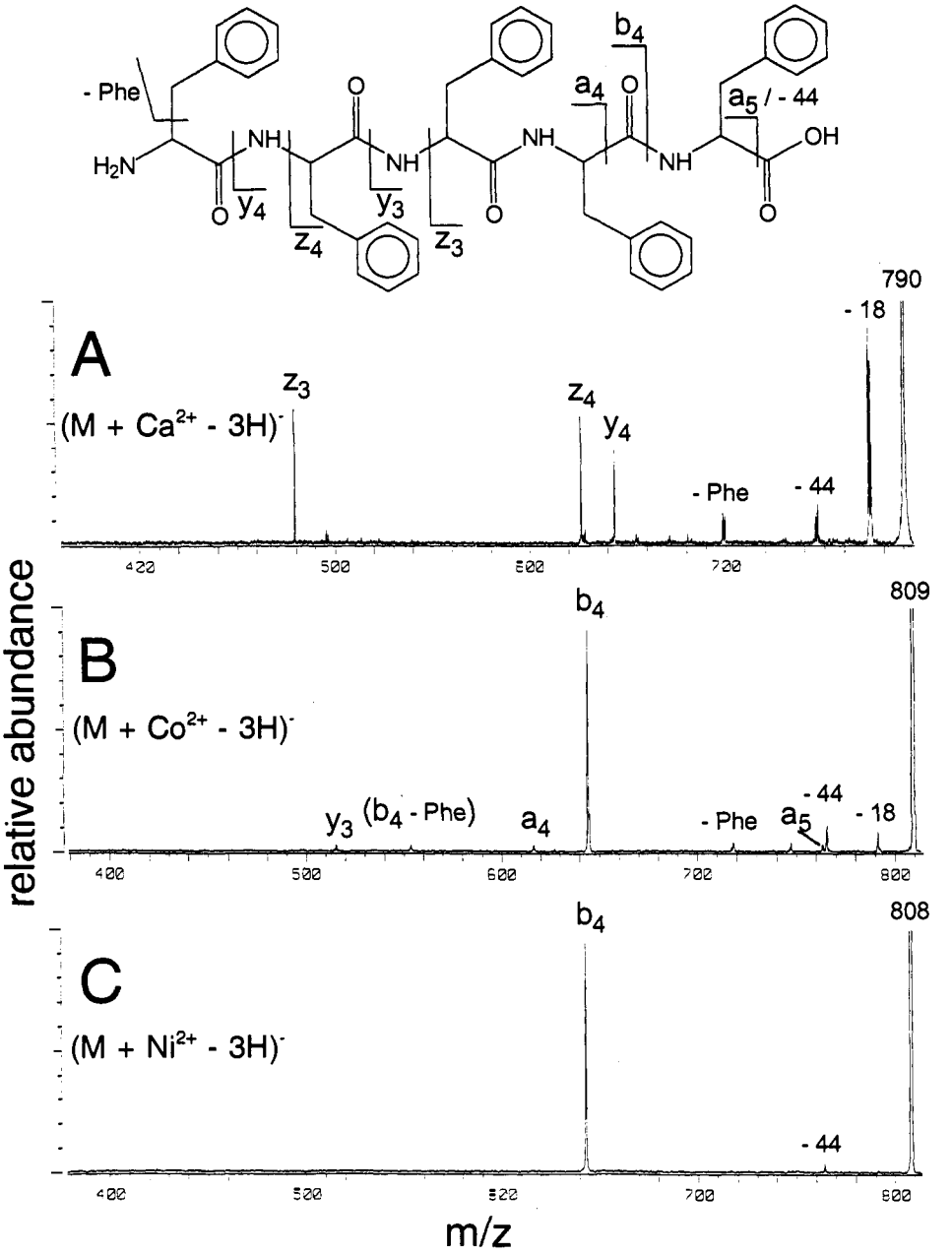

Figure 2. Metastable ion decomposition spectra of (A) $(M + Ca^{2+} - 3H)^-$, (B) $(M + Co^{2+} - 3H)^-$, and (C) $(M + Ni^{2+} - 3H)^-$ complexes of Phe-Phe-Phe-Phe-Phe. Ions labeled y_{n-m} and z_{n-m} are $(y_{n-m} + Cat^{2+} - 2H)^-$ and $(z_{n-m} + Ca^{2+} - 4H)^-$ ions, respectively. Ions labeled a_{n-m} and b_4 are $(a_{n-m} + Co^{2+} - 4H)^-$ and $(b_4 + Cat^{2+} - 4H)^-$ ions, respectively. Loss of the Phe side chain as either C_7H_8 in Figure 2A or $C_7H_7^\bullet$ in Figure 2A,B is labeled as –Phe. Ions labeled $(b_4 - Phe)$ are $(b_4 + Co^{2+} - 4H - Phe)^-$ ions, in which Phe indicates the loss of one Phe side chain as $C_7H_7^\bullet$.

the three deprotonated amides (structure **1a**) or the carboxylate, the adjacent deprotonated amide, and the distal deprotonated amide (structure **1b**). N-terminal product complexes, such as $(c_3 + Cat^{2+} - 2H)^-$ ions for Co^{2+} and Ni^{2+} (Figure 1B,C, respectively), usually only occur for Ca^{2+} in cases in which a protic amino acid side chain deprotonates and binds to the metal ion.[16]

Spectra in Figures 1 and 2, and spectra of five other tetra- through pentapeptides (Table 1), reveal the significantly different intrinsic binding preferences of the transition metal ions. The most striking feature of decompositions of Co^{2+} and Ni^{2+} complexes is the predominance of N-terminal ions. Tetrapeptide complexes primarily lose 44 as CO_2 from the free carboxylate terminus (Figure 1B,C, Table 1). Pentapeptide complexes primarily give $(b_4 + Cat^{2+} - 4H)^-$ ions (Figure 2B,C, Table 1).

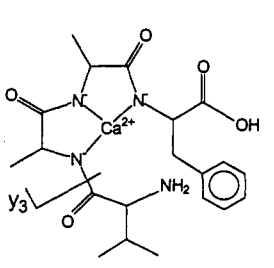

$(VAAF + Ca - 3H)^-$

Structure 1a

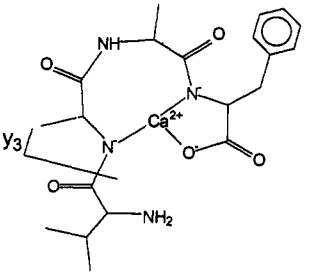

$(VAAF + Ca - 3H)^-$

Structure 1b

Spectra of VAAF in Figure 1 exemplify the decompositions of complexes between Co^{2+} and Ni^{2+} and tetrapeptides. Cleavages of the C-terminus involve losses of 44 as CO_2, HCO_2H to give

(19) The nomenclature for the sequence ions followed that presented in our previous[15,16] papers. For example, the designation of the $(y_3 + Ca^{2+} - 2H)^-$ ions gives the mass of the product ion formed by cleavage of the amide bond of the third amino acid from the C-terminus with transfer of hydrogen to the product ion.

Table 1. Relative Ion Abundance (%) in Metastable Ion Decomposition Spectra of Complexes of Hydrocarbon Peptides[a]

		c_3	a_4	b_4	x_2	y_2	x_3	y_3	z_3	y_4	z_4	−44
AGFL												
	Ca^{2+}						0.56	1.31				0.34
	Co^{2+}	0.49	0.61			0.73						1.50
	Ni^{2+}	0.72										2.71
ALAL												
	Ca^{2+}	0.22					0.28	1.58				0.25
	Co^{2+}	0.74	0.40			0.28						1.97
	Ni^{2+}	0.45										2.33
FFFF												
	Ca^{2+}						0.33	0.40	0.27			
	Co^{2+}	0.23	0.39			0.12						2.97
	Ni^{2+}											3.17
VAAF												
	Ca^{2+}				0.02			0.37				0.09
	Co^{2+}	0.09	0.23			0.08						3.04
	Ni^{2+}	0.08										2.60
FFFFF												
	Ca^{2+}							0.02	0.18	0.13	0.17	0.06
	Co^{2+}		0.07	1.86				0.06				0.22
	Ni^{2+}			4.72								0.18
FFGLM-NH_2												
	Ca^{2+}										0.31	
	Co^{2+}		0.30	0.20		0.02		0.09	0.04			
	Ni^{2+}		0.26	0.71								
GAAAA												
	Ca^{2+}						0.24	0.43	0.70	0.16	0.14	0.27
	Co^{2+}			5.92				0.58				
	Ni^{2+}			5.62								

[a] Relative abundances are reported relative to the main beam for ions that appear at greater than twice the S/N.

Scheme 1

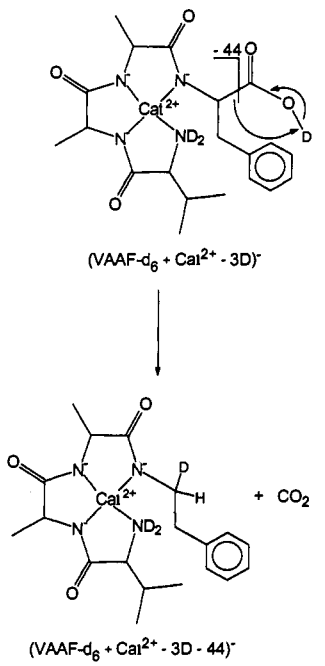

$(a_4 + Co^{2+} - 4H)^+$ ions, and portions of the C-terminal amino acid to give $(c_3 + Cat^{2+} - 2H)^+$ ions. The only energetically reasonable precursor structure that can give the ions is one in which three deprotonated amides bind Co^{2+} and Ni^{2+}. Theory says that the most intrinsically stable configuration has the metal ion also bound to the N-terminal amine in a square-planar complex (Scheme 1).[20] Decompositions of $(VAAF\text{-}d_6 + Co^{2+} - 3D)^+$ complexes also give loss of 44, supporting the mechanism in Scheme 1. The precursor structure is analogous to aqueous- and solid-phase structures of Ni^{2+}–tetrapeptide complexes.[3] All product ion complexes are square-planar.

(20) Huheey, J. E. *Inorganic Chemistry*, 3rd ed.; Harper & Row: New York, 1983; pp 359–463.

Scheme 2

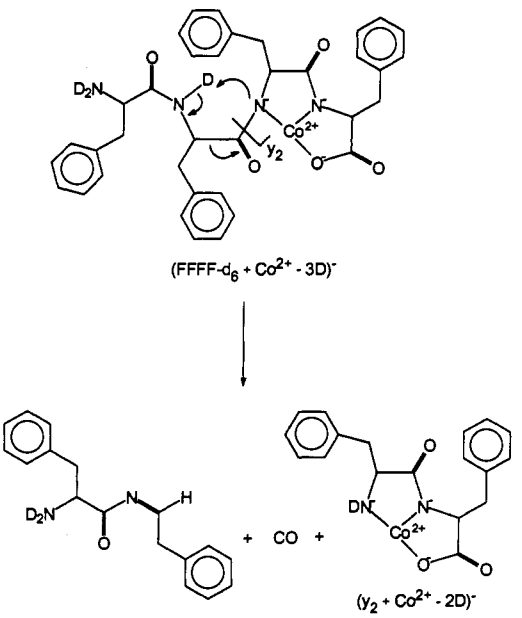

The ionization process also forms some less favorable, and less abundant, Co^{2+}-tetrapeptide complexes, species that are not seen in solution. They decompose to give weakly abundant C-terminal $(y_2 + Co^{2+} - 2H)^+$ ions (Table 1). Decompositions of $(FFFF\text{-}d_6 + Co^{2+} - 3D)^+$ complexes indicate that the products arise from an intrinsically unfavorable[20] tricoordinate structure in which the carboxylate and two adjacent deprotonated amides bind Co^{2+} (Scheme 2). The products also have an intrinsically unfavorable[20] tricoordinate structure. Semiempirical calculations for the Co^{2+}–VAAF complex analogous to the one shown in Scheme 2 do not reveal binding interactions between the metal ion and any other functional group.

No Ni^{2+} complexes decompose to give products that contain Ni^{2+} bound to the C-terminus (Figure 1C, Table 1). This shows that formation of C-terminal Ni^{2+} precursors is less favorable than formation of C-terminal Co^{2+} precursors. Consequently,

Scheme 3

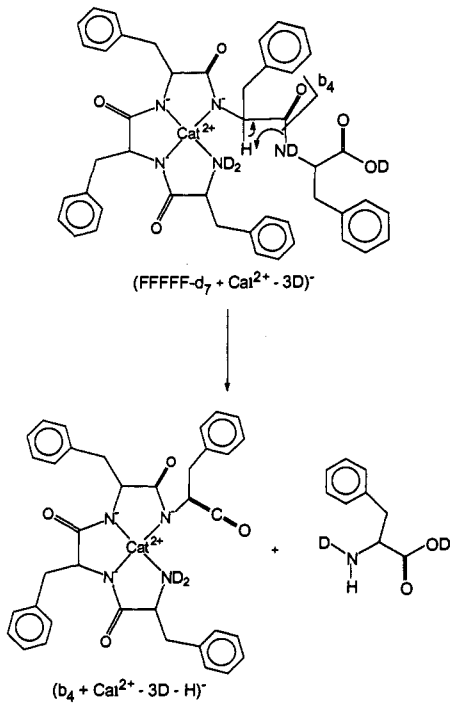

Scheme 4

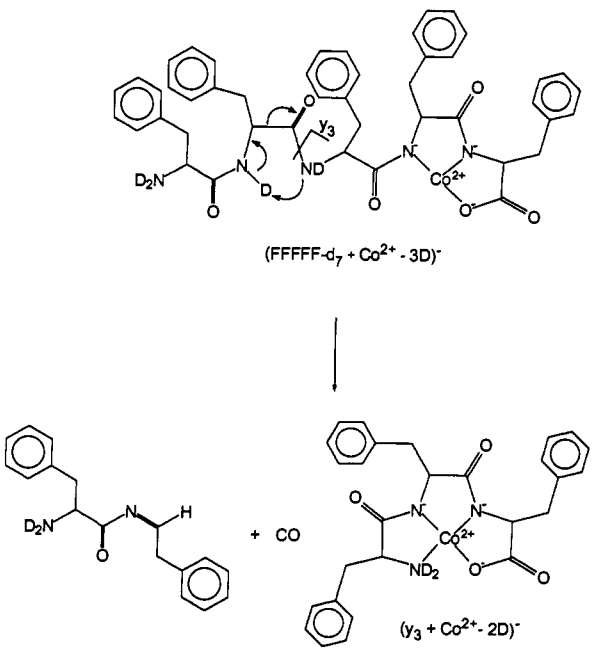

Ni^{2+} has an intrinsically stronger preference than Co^{2+} for binding to the N-terminus.

Spectra of the exemplary pentapeptide FFFFF (Figure 2 and Table 1) also show different binding preferences of Ca^{2+}, Co^{2+}, and Ni^{2+}. Ca^{2+} complexes decompose to give highly abundant C-terminal sequence ions in which Ca^{2+} is bound toward the C-terminus (Figure 2A and Table 1). In sharp contrast, Co^{2+} and Ni^{2+} complexes primarily give highly abundant N-terminal $(b_4 + Cat^{2+} - 4H)^-$ ions (Figure 2B,C, Table 1). Co^{2+} complexes also undergo other reactions to give a variety of weakly abundant products.

A square-planar precursor complex (Scheme 3) analogous to the one in Scheme 1 is the only intrinsically stable structure from which the N-terminal product complexes can arise. The products also are square-planar. Decompositions of (FFFFF-d_7 + Co^{2+} – 3D)$^-$ complexes give products that contain two deuteriums, in support of the mechanism. Co^{2+} and Ni^{2+} complexes of all pentapeptides studied (Table 1) give $(b_4 + Cat^{2+} - 4H)^-$ products as the most abundant N-terminal ions. Other peptide complexes of GGFM, GGYFM, GYGFM, YGGFL, YGGFH, HLGLAR, LHGLAR, LGHLAR, SGAGAG, DRVYIHPF, Sar-RVYI-HPF, RVYVHPF, DTHAAA, and ADTHAA similarly give abundant $(b_4 + Cat^{2+} - 4H)^-$ ions, at least for Ni^{2+}. The chemistry of these peptides that contain special side chains will be discussed in a later paper. Cleavages to give $(b_4 + Cat^{2+} - 4H)^-$ ions are in immediate proximity to the metal ion binding site and reveal the exact location of the metal ion. The high abundances of the products reveal the preferential formation of them and their precursors. Ni^{2+} complexes generally give significantly higher total abundances of N-terminal ions, and always form more abundant $(b_4 + Ni^{2+} - 4H)^-$ ions, than Co^{2+} complexes (Table 1). This shows the intrinsically stronger preference of Ni^{2+} for binding to the N-terminus.

Less-favored Co^{2+} complexes of the pentapeptide FFFFF decompose to give weakly abundant C-terminal $(y_3 + Co^{2+} - 2H)^-$ ions (Figure 2B, Table 1). Decompositions of (FFFFF-d_7 + Co^{2+} – 3D)$^-$ complexes indicate that $(y_3 + Co^{2+} - 2H)^-$ ions arise from unfavorable tricoordinate precursors that give favorable, stable square-planar product ions (Scheme 4). Semiempirical calculations were not performed for the FFFFF complexes. In analogy to VAAF, however, it is unlikely that the metal ion interacts with other functional groups besides the deprotonated carboxylate and amides. The products are structurally analogous to solution-phase complexes between tripeptides and Ni^{2+}.[3a,e] Reaction from a thermodynamically unfavorable reactant to a highly thermodynamically stable product is exoergic and kinetically favorable near the threshold. Co^{2+} complexes of all pentapeptides studied (Table 1) give weakly abundant $(y_3 + Co^{2+} - 2H)^-$ ions.

No Ni^{2+} complexes of tetra- and pentapeptides give either $(y_3 + Ni^{2+} - 2H)^-$ or any other C-terminal sequence ions (Table 1). The only exceptions are cases in which N-terminal binding of the metal ion is prohibited, which will be discussed in the next section. Other exceptions occur when there is an amino acid located toward the C-terminus, such as Met or His, that can bind the metal ion. This chemistry will be discussed in a later paper. Data for the hydrocarbon peptides show that Ni^{2+} intrinsically prefers binding to the N-terminus more than Co^{2+}.

In summary, data for the hydrocarbon peptides (Table 1) reveal that in contrast to Ca^{2+}, which preferentially complexes toward the C-terminus, Co^{2+} and Ni^{2+} preferentially bind the N-terminal amine. The data also reveal the following: (1) Ca^{2+} does not bind to the N-terminal amine. (2) Co^{2+} preferentially binds to the N-terminus, but it can bind to the C-terminal carboxylate. (3) Ni^{2+} prefers to bind exclusively to the N-terminal amine. (4) Hydrocarbon amino acid side chains, excluding Pro, in tetrapeptides and larger peptides do not affect formation of square-planar N-terminal Co^{2+} and Ni^{2+} complexes.

Binding of Co^{2+} and Ni^{2+} to Tripeptides That Contain Hydrocarbon Amino Acid Side Chains. Extension of the peptide backbone from tetrapeptides to larger peptides does not alter formation of either intrinsically favored N-terminal square-planar precursor or product ion complexes. Tripeptides also form thermodynamically stable square-planar precursors (structure **2**). The complexes, however, do not decompose to reveal this intrinsically favored binding interaction.

For example, Ni^{2+} complexes of FFF (Figure 3A) lose CO_2, HCO_2H to give N-terminal $(a_3 + Ni^{2+} - 4H)^-$ ions, and both CO_2 and one Phe side chain as $(- 44 - C_7H_7^{\bullet})$. Each reaction cleaves bonds in the stable and favored square-planar structure **2**. Another alternative involves cleavage of an intrinsically unfavored tricoordinate complex (structure **3**). Either possibility gives unfavored tricoordinate products. It is impossible to know whether the reactions arise either directly from structure **2** with

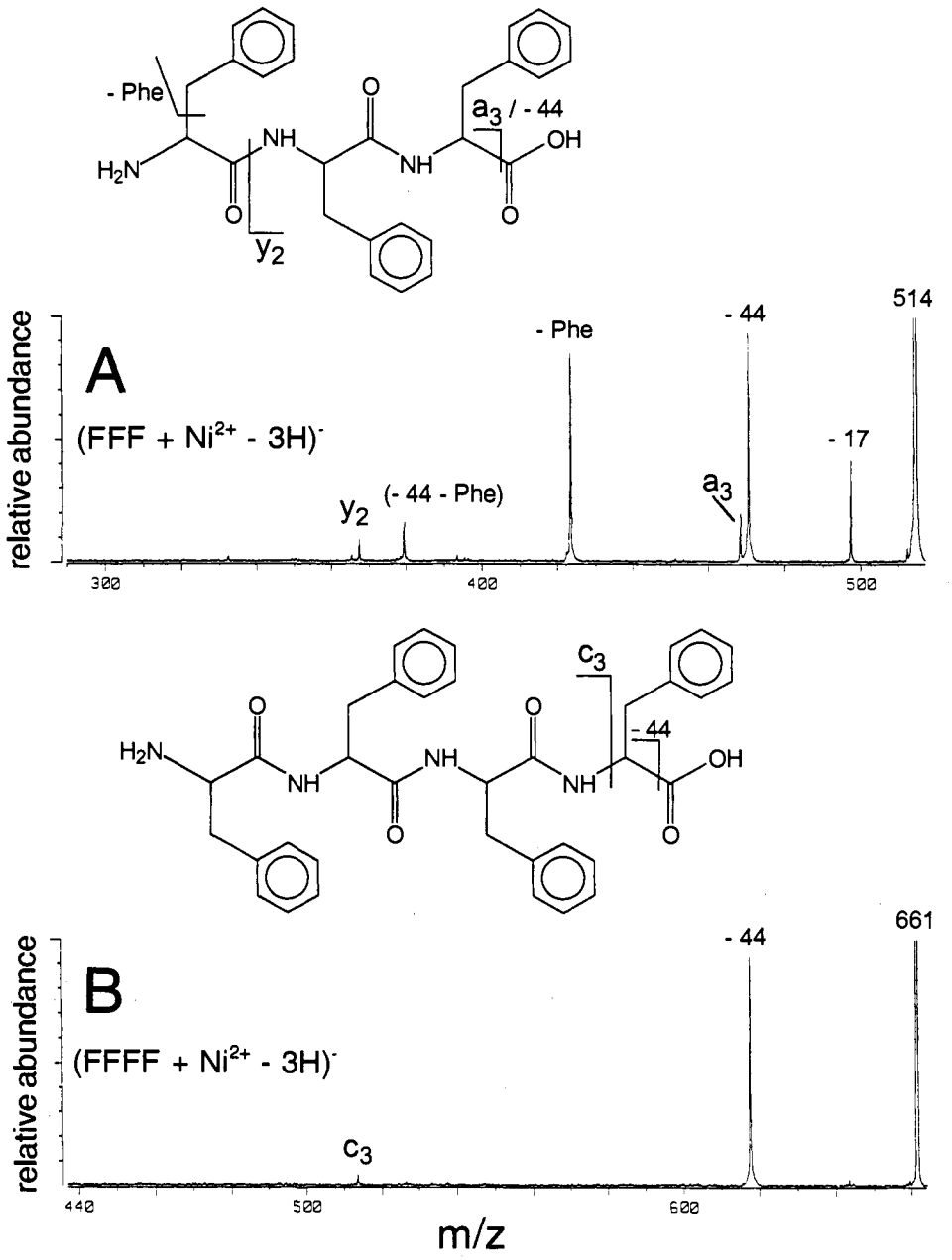

Figure 3. Metastable ion decomposition spectra of $(M + Ni^{2+} - 3H)^-$ complexes of (A) Phe-Phe-Phe and (B) Phe-Phe-Phe-Phe. Ions labeled y_2 are $(y_2 + Ni^{2+} - 2H)^-$ ions. Ions labeled a_3 and c_3 are $(a_3 + Ni^{2+} - 4H)^-$ and $(c_3 + Ni^{2+} - 2H)^-$ ions, respectively. Loss of one Phe side chain as $C_7H_7^\bullet$ is labeled as –Phe. Ions labeled (– 44 – Phe) are formed by losses of both CO_2 and a Phe side chain as $C_7H_7^\bullet$.

concomitant cleavage of the Ni^{2+}–O^- chelate bond or instead from the less stable structure **3**.

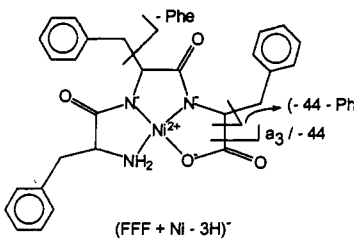

Structure 2

More obvious precursor structures give other product ions. C-terminal $(y_2 + Ni^{2+} - 2H)^-$ ions (Figure 3A) are tricoordinate and arise from tricoordinate precursors in which the carboxylate and two deprotonated amides bind Ni^{2+}, as for Co^{2+} and FFFF in Scheme 2. The only reactions that occur from the intrinsically

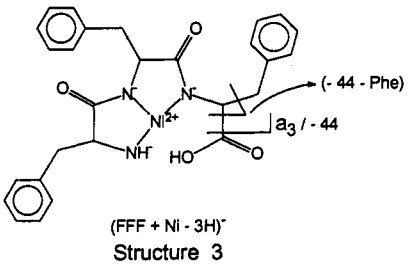

Structure 3

favored structure **2** to give intrinsically favored square-planar products are losses of side chains, such as $C_7H_7^\bullet$ (–Phe) (Figure 3A).

In contrast to tripeptides, lower energy reaction channels are available for FFFF (Figure 3B) and FFFFF (Figure 2C) precursors that leave the stable, square-planar complex intact in the products. Relative product ion abundances (Table 2) reveal the inherent stability and resistance to cleavage of the tetracoordinate precursors. For the tripeptide, losses of CO_2 and $C_7H_7^\bullet$

Table 2. Relative Abundances (%) in Metastable Ion Decomposition Spectra of $(M + Ni^{2+} - 3H)^-$ Complexes[a]

	a_3	c_3	b_4	y_2	$(-CO_2 - Phe)^b$	$-CO_2$	$-Phe^b$	−17	total
FFF	0.06			0.03	0.05	0.26	0.24	0.12	0.76
FFFF		0.10				1.8			1.9
FFFFF			4.7			0.18			4.9

[a] Relative abundances are reported relative to the main beam for ions that appear at greater than twice the S/N. [b] Phe indicates loss of a Phe side chain as $C_7H_7^{\bullet}$.

are comparably probable. In contrast, the most probable reaction of FFFF is loss of CO_2 and that of FFFFF is formation of $(b_4 + Ni^{2+} - 4H)^-$ ions. Relative abundances of the later two decompositions are significantly greater than the abundances of products from FFF. Disruption of the FFF square-planar complex is less facile than the low-energy cleavages of the FFFF and FFFFF backbones, neither of which requires disrupting the stable square-planar chelate nor directly homolytically cleaving a side chain. These facile reactions of tetrapeptides and larger peptides, which occur in immediate proximity to the metal ion binding site, unequivocally reveal the intrinsically preferred coordination of the metal ion in both precursor and product.

Binding Interactions with Peptides That Contain Pro (P). The above data give important information about some intrinsic binding features of the complexes. Studies of peptides that contain Pro provide information about intrinsic geometric constraints. The structure of Pro precludes deprotonation of its amide so that no metal ion–N^- bond can be formed. Thus, the presence of Pro significantly alters the coordinating properties of a peptide.

N-terminal Pro does not inhibit formation of square-planar, N-terminal Co^{2+} and Ni^{2+} precursors. For example, Co^{2+} and Ni^{2+} complexes of PFGK decompose similarly to those of VAAF (Table 3) and are structurally similar to the complex shown in Scheme 1. The N-terminal secondary amine of the Pro residue, however, and the three deprotonated amides bind the metal ion. This chemistry is analogous to aqueous binding interactions between peptides that contain a N-terminal Pro and Ni^{2+} and Cu^{2+}.[4,5]

Pro as the second to fourth amino acid from the N-terminus does not inhibit formation of N-terminal Ca^{2+} complexes because Ca^{2+} can bind to an N-terminal deprotonated side chain (YPFAG and ADVPAA in Table 3).[16] For example, abundant $(c_3 + Ca^{2+} - 2H)^-$ ions arise from Ca^{2+} binding to the deprotonated Tyr (Y) side chain and the two deprotonated amides on the C-terminal side of Pro in YPFAG (Figure 4A).[16a]

In contrast, Pro as the second to fourth amino acid from the N-terminus inhibits formation of the normal N-terminal complexes for Co^{2+} and Ni^{2+} (Table 3). Unless there is a specific side chain that can bind the metal ion toward the N-terminus, the peptides only form C-terminal complexes. YPFAG complexes of Co^{2+} and Ni^{2+} exemplify this chemistry (Figure 4B,C). The $(y_3 + Cat^{2+} - 2H)^-$ ions arise via an exoergic reaction analogous to Scheme 4. The less abundant $(y_4 + Ni^{2+} - 2H)^-$ ions only occur for some peptides that contain Pro (compare Table 1 to Table 3). Interestingly, the Ni^{2+}-containing ions are of greater abundances than their undetected Co^{2+} counterparts only for YPFAG. Decompositions of $(YPFAG\text{-}d_7 + Ni^{2+} - 3D)^-$ complexes indicate that the $(y_4 + Ni^{2+} - 2H)^-$ ions arise from an exoergic reaction in which less stable tricoordinate precursors give stable square-planar products (Scheme 5). The $(y_4 + Ni^{2+} - 2H)^-$ ions also arise via an equally probable mechanism in which the N-terminal amine transfers a deuterium. This is consistent with our previous results[21] that show that reaction mechanisms depend on peptide structure. The MS–MS–MS (MS^3) spectrum of the $(y_4 + Ni^{2+} - 2H)^-$ ions shows abundant loss of CO_2, which supports the proposed structure of the product ions. The product ions, which contain Ni^{2+} strongly bonded to N ligands, are analogous to solution-phase complexes between PGGG and Ni^{2+}.[4] Thus, Pro as the fourth amino acid from the C-terminus is also an important feature of this peptide. The greater intrinsic preference of Ni^{2+} for forming the square-planar, N-terminal product complexes from YPFAG causes formation of more abundant $(y_4 + Ni^{2+} - 2H)^-$ ions vs their Co^{2+} counterparts.

The gas-phase chemistry of Pro as the third amino acid from the N-terminus is similar to that of YPFAG and similar to solution-phase chemistry. For example, Co^{2+} and Ni^{2+} complexes

Table 3. Relative Ion Abundances (%) in Metastable Ion Decomposition Spectra of Complexes of Peptides That Contain Pro[a]

		a_3	b_3	c_3	a_4	b_4	c_4	b_5	x_3	y_3	z_3	x_4	y_4	z_4	x_5	y_5	z_5	−44	−18
PFGK																			
	Ca^{2+}			0.17					0.11	0.18[b]	0.12								2.0
	Co^{2+}		0.02	0.09	0.18					0.03								0.66	0.29
	Ni^{2+}			0.28														1.4	
YPFAG																			
	Ca^{2+}			0.18							0.14		0.05					0.51	0.28
	Co^{2+}									3.7								0.13	0.28
	Ni^{2+}									0.81			0.24					0.22	0.06
ADVPAA																			
	Ca^{2+}						0.12					0.16					0.27	0.10	2.2
	Co^{2+}							0.04		0.66			0.30					0.05	1.0
	Ni^{2+}							0.07	0.06	0.55			0.10					0.48	0.18
AAAPAA																			
	Ca^{2+}									0.01		0.25	0.14	0.06		0.05	0.01	0.06	0.34
	Co^{2+}								0.02	0.12			0.05					0.02	
	Ni^{2+}								0.02	0.07			0.03					0.05	0.02
VGVAPG																			
	Ca^{2+}								0.05				0.47		0.08	0.14		0.99	1.1
	Co^{2+}				0.05	1.1							0.05					0.29	0.17
	Ni^{2+}					1.9												0.16	0.06
VHLGP																			
	Ca^{2+}			0.01		0.07							0.08	0.33				0.52	0.35
	Co^{2+}				0.02	2.9												0.14	0.08
	Ni^{2+}					4.0												0.08	
AADVPA																			
	Ca^{2+}								0.03				0.06	0.09		0.07		0.22	0.81
	Co^{2+}					0.89[c]							0.03	0.13				0.12	1.1
	Ni^{2+}	0.02	0.03			0.45[c]										0.03		0.12	0.21

[a] Relative abundances are reported relative to the main beam for ions that appear at greater than twice the S/N. [b] This is actually the $(y_3 - Phe)$ ion. [c] This is the sum of the abundances of the b_4 ions plus $(b_4 - CO_2)$ ions.

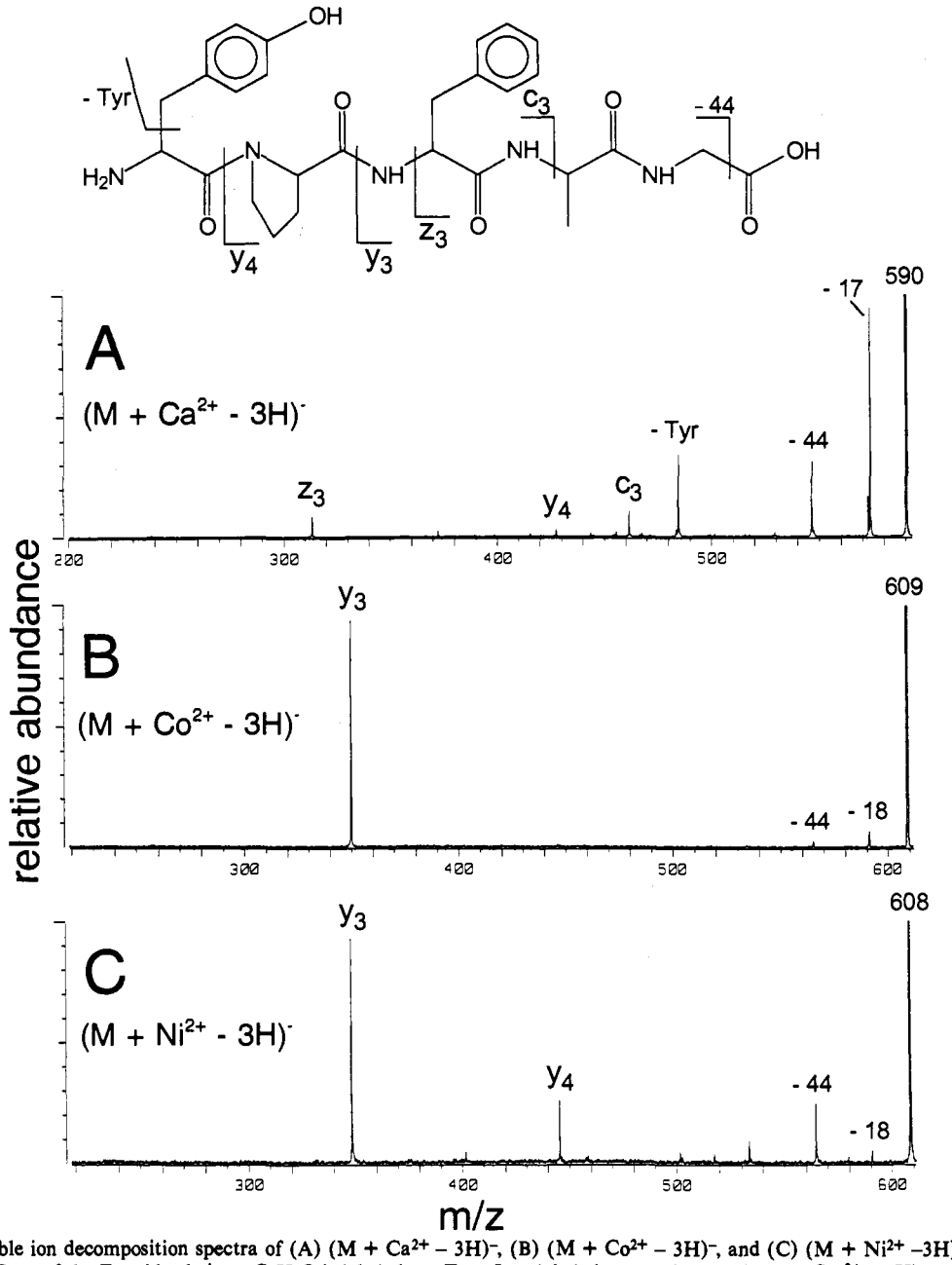

Figure 4. Metastable ion decomposition spectra of (A) $(M + Ca^{2+} - 3H)^-$, (B) $(M + Co^{2+} - 3H)^-$, and (C) $(M + Ni^{2+} - 3H)^-$ complexes of Tyr-Pro-Phe-Ala-Gly. Loss of the Tyr side chain as C_7H_6O is labeled as –Tyr. Ions labeled y_{n-m} and z_3 are $(y_{n-m} + Cat^{2+} - 2H)^-$ and $(z_3 + Ca^{2+} - 4H)^-$ ions. Ions labeled c_3 are $(c_3 + Ca^{2+} - 2H)^-$ ions.

of ADVPAA also give abundant $(y_3 + Cat^{2+} - 2H)^-$ ions (Table 3). Decompositions of (ADVPAA-d_8 + Co^{2+} – 3D)$^-$ complexes indicate that the $(y_3 + Cat^{2+} - 2H)^-$ ions are analogous to $(y_4 + Ni^{2+} - 2H)^-$ ions of YPFAG. Both peptide complexes give a new peptide that contains Pro as the N-terminus (compare Scheme 5 to Scheme 6). The exoergic reaction of unfavorable tricoordinate precursors gives stable, square-planar, products. The products from ADVPAA are analogous to solution-phase complexes between Ni^{2+} and PGG and PLG-NH_2.[4,5] Thus, Pro as the third amino acid from the C-terminus is also an important feature of this peptide. Decompositions of (ADVPAA-d_8 + Co^{2+} – 3D)$^-$ complexes reveal another exoergic reaction that gives less abundant tetracoordinate $(y_4 + Cat^{2+} - 2H)^-$ products (Scheme 7). These products contain an eight-membered, highly distorted square-planar chelate ring. The products are analogous to solution-phase complexes between Cu^{2+} and GPGG and APAA.[6,7]

The products are less stable and the reaction less exoergic than depicted in Scheme 6 for the $(y_3 + Cat^{2+} - 2H)^-$ ions, however. This is particularly the case for Ni^{2+}, which intrinsically prefers to form rigid square-planar complexes more than Co^{2+}.[20] Consequently, the $(y_4 + Ni^{2+} - 2H)^-$ ions are less abundant than their Co^{2+} counterparts.

The chemistry of complexes that contain Pro as either the first or second amino acid from the C-terminus also reveals structural requirements for metal ion binding. One example is VGVAPG (Table 3 and Figure 5), in which Ca^{2+} forms a variety of C-terminal sequence ions. The abundant $(y_4 + Ca^{2+} - 2H)^-$ ions (Figure 5A) arise from complexes in which three deprotonated sites that are separated by Pro bind Ca^{2+}.[16c] In contrast, the most abundant ions for Co^{2+} (Figure 5B) and Ni^{2+} (Figure 5C) are the typical N-terminal $(b_4 + Cat^{2+} - 4H)^-$ ions. The data reveal that Ca^{2+} can form flexible but Co^{2+} and Ni^{2+} prefer to form square-planar complexes.

Interestingly, there are some weakly abundant C-terminal $(y_4 + Co^{2+} - 2H)^-$ ions that do not have Ni^{2+} counterparts (Figure

(21) Zhao, H.; Adams, J. *Int. J. Mass Spectrom. Ion Processes* **1993**, *125*, 195–205.
(22) Anderson, W. P.; Edwards, W. D.; Zerner, M. C. *Inorg. Chem.* **1986**, *25*, 2728–2732.

Scheme 5

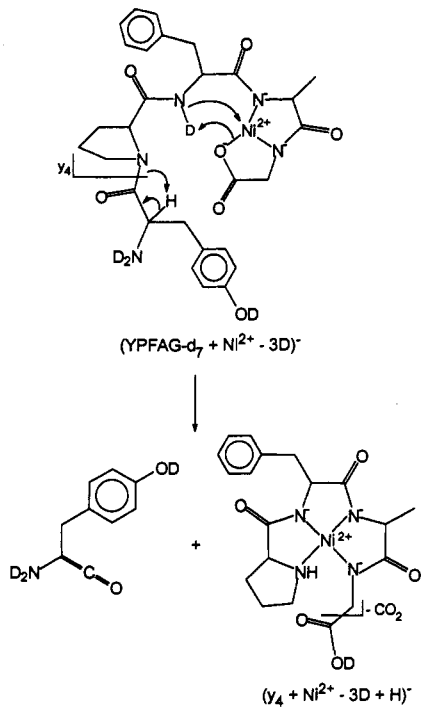

Scheme 6

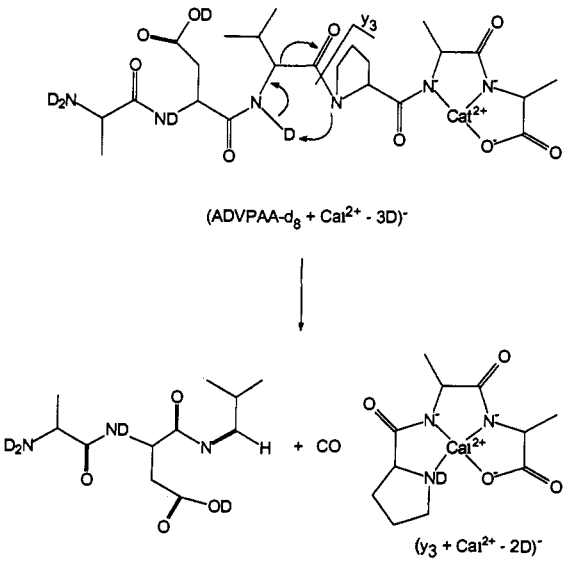

5B,C, Table 3). These unfavorable products arise from weakly abundant precursors which, as for Ca^{2+}, contain Co^{2+} bound to three deprotonated sites that are separated by Pro. Decompositions of (VGVAPG-d_7 + Co^{2+} – 3D)$^-$ complexes reveal an exoergic reaction of tricoordinate precursors to give highly distorted square-planar products (Scheme 8). The products are analogous to solution-phase complexes between Cu^{2+} and GGPA and AAPA.[7] Thus, Pro as the second amino acid from the C-terminus is an important feature of this peptide. The difference between Co^{2+} and Ni^{2+} shows that Ni^{2+} more strongly prefers forming square-planar, as opposed to distorted square-planar, complexes than Co^{2+}.

Metal-Ion-Specific Binding Sites. There is one peptide in Table 3, AADVPA, in which the Ni^{2+} complexes decompose unusually. Ca^{2+} and Co^{2+} complexes react similarly to VGVAPG except they also lose the Asp (D) side chain. Co^{2+} complexes also give weakly abundant C-terminal (z_4 + Co^{2+} – 4H)$^-$ ions. An unfavorable tricoordinate complex in which the Ca^{2+}-specific binding sequence -Asp-Val-Pro- (-DVP-)[11] binds Co^{2+} can give

Scheme 7

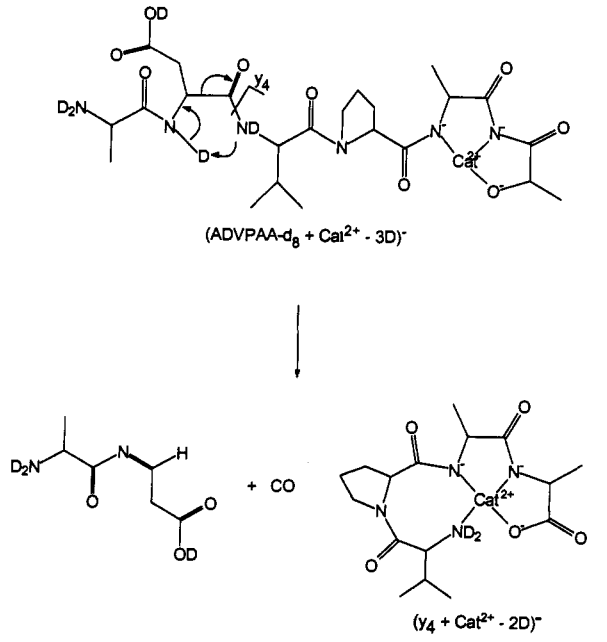

the ions (structure **4**).[16c] The Ni^{2+} complexes are unusual because they give weakly abundant N-terminal (a_3 + Ni^{2+} – 4H)$^-$ and (b_3 + Ni^{2+} – 4H)$^-$ ions and they do not lose the Asp side chain.

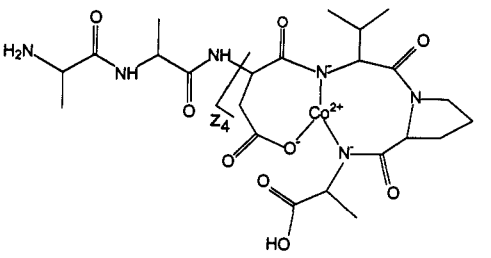

(AADVPA + Co - 3H)$^-$
Structure 4

The data reveal an intrinsic Ni^{2+}-specific binding interaction with the Asp side chain. The interaction prevents its cleavage and gives the (a_3 + Ni^{2+} – 4H)$^-$ and (b_3 + Ni^{2+} – 4H)$^-$ ions. A tetracoordinate precursor in which the N-terminal amine, the two adjacent deprotonated amides, and the deprotonated Asp side chain carboxylate bind Ni^{2+} explains the chemistry (structure **5**). This specific binding interaction with Asp as the third amino acid from the N-terminus also occurs in the aqueous phase.[8,9] It is also similar to solution-phase chemistry of complexes that contain His,[10] which will be discussed in a later paper.

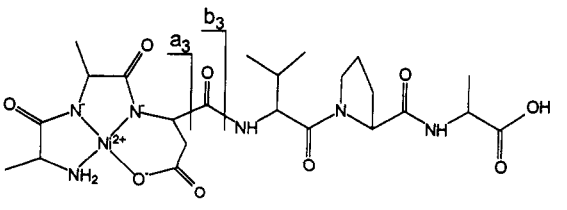

(AADVPA + Ni - 3H)$^-$
Structure 5

We[16c] recently showed that the Ca^{2+}-specific -DVP- binding sequence in staphylococcal nuclease is also specific for Ca^{2+} in the gas phase. Ca^{2+} intrinsically prefers to bind across the -DVP- sequence, whereas Mg^{2+} and Ba^{2+} do not. The same specificity for Ca^{2+} vs the two transition metal ions occurs here. Ca^{2+} binds

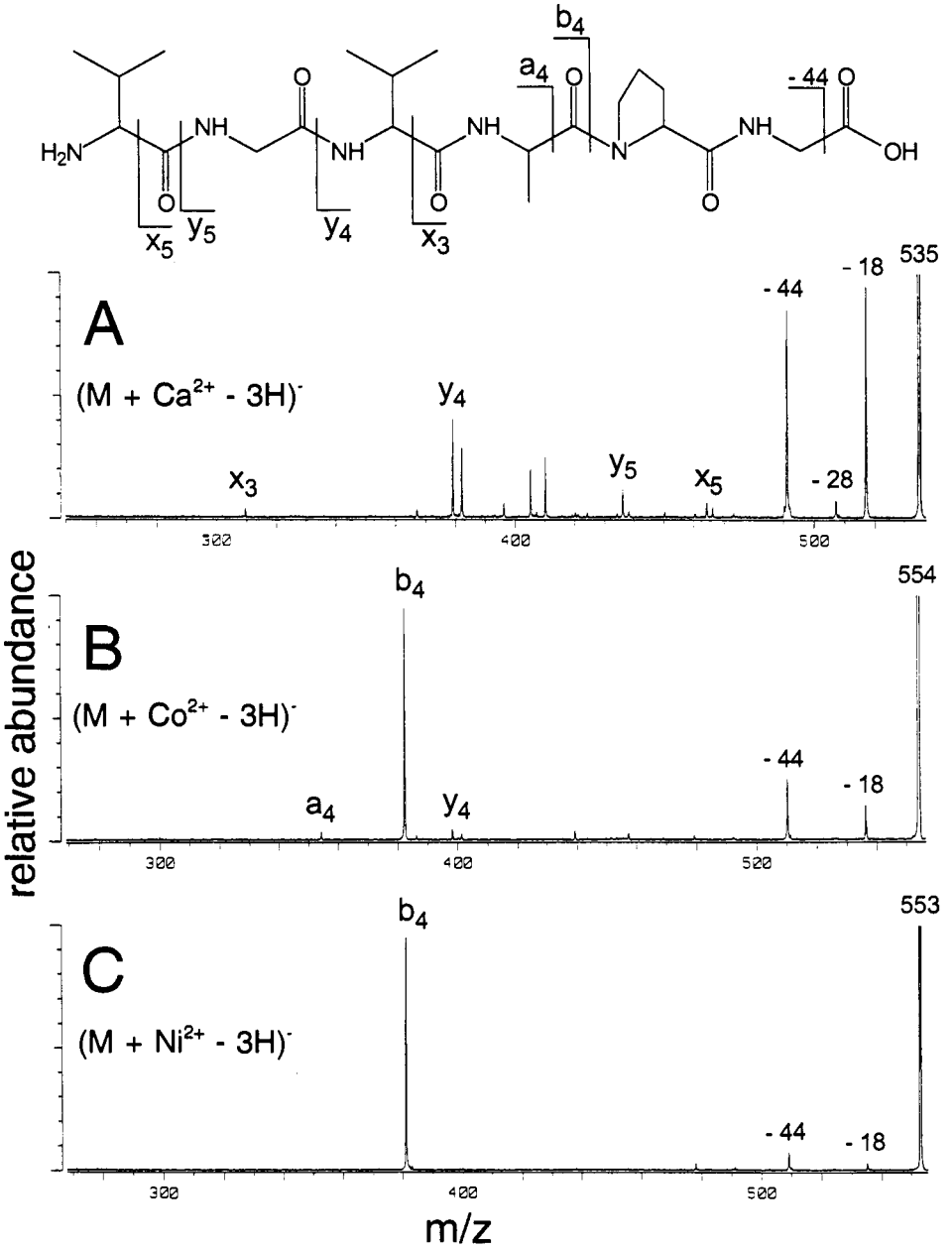

Figure 5. Metastable ion decomposition spectra of (A) $(M + Ca^{2+} - 3H)^-$, (B) $(M + Co^{2+} - 3H)^-$, and (C) $(M + Ni^{2+} - 3H)^-$ complexes of Val-Gly-Val-Ala-Pro-Gly. Ions labeled x_{n-m} and y_{n-m} are $(x_{n-m} + Ca^{2+} - 2H)^-$ and $(y_{n-m} + Cat^{2+} - 2H)^-$ ions, respectively. Ions labeled a_4 and b_4 are $(a_4 + Co^{2+} - 4H)^-$ and $(b_4 + Cat^{2+} - 4H)^-$ ions, respectively.

across the -DVP- sequence in ADVPAA to give abudnant $(c_4 + Ca^{2+} - 2H)^-$ and $(z_5 + Ca^{2+} - 4H)^-$ ions (Table 3). Significantly less favorable Co^{2+} and Ni^{2+} complexes that involve the -DVP- binding site give weakly abundant $(b_5 + Cat^{2+} - 4H)^-$ ions. These ions are 1 order of magnitude less favorable than others in the spectra. Ca^{2+} similarly binds across -DVP- in AADVPA to give abundant $(z_4 + Ca^{2+} - 4H)^-$ ions. Co^{2+} complexes also give these ions, but they are significantly less abundant than the preferentially formed $(b_4 + Co^{2+} - 4H)^-$ ions. The Ni^{2+} complexes give no $(z_4 + Ni^{2+} - 4H)^-$ ions but instead strongly prefer to form N-terminal square-planar species.

Discussion

Binding interactions between Ni^{2+} and peptides have been studied extensively in the aqueous and solid phases. Ni^{2+} forms octahedral bis-complexes with dipeptides that contain hydrocarbon amino acids, in which both peptides function as tridentate ligands. The N-terminal amines, deprotonated amide(s), and C-terminal carboxylate(s) strongly bind the metal ion.[12] Ni^{2+} exclusively forms square-planar complexes with larger peptides that contain hydrocarbon amino acids, however.[3] In tripeptides, the N-terminal amine, the two deprotonated amides, and the C-terminal carboxylate strongly bind Ni^{2+}.[3a] In tetrapeptides and larger peptides that contain hydrocarbon amino acids, the N-terminal amine and the three adjacent deprotonated amides strongly bind Ni^{2+}.[3] These binding interactions form a highly stable, square-planar complex. Any potential binding sites created by further extension of the peptide backbone do not give additional Ni^{2+}–N^- bonds because the resulting square pyramidal complex is intrinsically less stable.[3e,3f,20] Peptides that have N-terminal Pro bind to metal ions such as Ni^{2+} and Cu^{2+} in ways similar to peptides that do not contain Pro.[4,5] Peptides that have Pro at other positions, however, have different binding interactions. Larger than five-membered chelate rings form geometries that are less stable than square-planar.[6,7]

Solution- and solid-phase studies show that Co^{2+} binds differently than Ni^{2+} to larger peptides. Co^{2+} forms octahedral bis-complexes with dipeptides, similarly to Ni^{2+}.[13] Co^{2+}, however,

Scheme 8

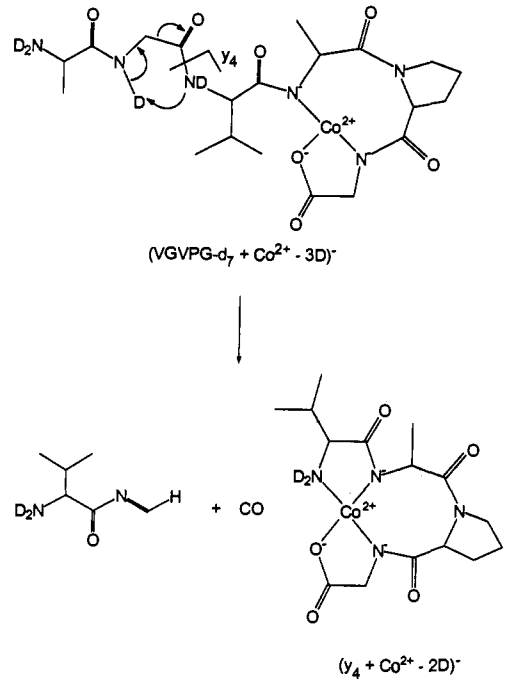

forms octahedral bis-complexes with tripeptides, which is different from Ni^{2+} that prefers square-planar complexes.[13] Co^{2+} also prefers to form tetrahedral complexes. With multidentate ligands such as peptides, however, it can be forced into square-planar geometry.

Ca^{2+} binds totally differently from the transition metal ions. Aqueous- and solid-phase studies show that Ca^{2+} binds to peptides via ether the C-terminal carboxylate, the amide carbonyl oxygens, and/or the side-chain hydroxyl or carboxylate oxygens.[14] Ca^{2+} prefers to form flexible complexes with variable bond lengths. Ca^{2+} does not substitute for an amide proton in aqueous solution. Instead, Ca^{2+} precipitates as its hydroxide before amide deprotonation occurs.

The aqueous- and solid-phase chemistry is understood from ligand field, crystal field, and molecular orbital theories that address intrinsic binding features of the metal ions.[20] Theory says that Ni^{2+} strongly prefers binding to strong-field N ligands in a square-planar geometry. In contrast, Co^{2+} prefers N ligands less and O ligands more than Ni^{2+}. Co^{2+} can form complexes with either N or O ligands, however, in a variety of configurations, such as octahedral and tetrahedral. Ca^{2+} strong prefers O ligands and binds in a variety of flexible configurations with no clear geometric preferences.

Consequently, it is not surprising that the intrinsic gas-phase results for Co^{2+} and Ni^{2+} reflect theory and most aqueous-phase chemistry. The most abundant product ions from either hydrocarbon peptides or ones that contain an N-terminal Pro arise from, and are themselves, square-planar N-terminal complexes. The N-ligand products reflect abundantly formed precursors that contain the metal ions intrinsically bound in the same thermodynamically preferred geometry as in aqueous solution. Mass spectrometry, however, also detects less favorable Co^{2+} complexes from their weakly abundant C-terminal products. These C-terminal ions are missing in the spectra of the Ni^{2+} complexes. This difference results from Co^{2+} lacking a strong preference for either N or O ligands or a specific geometry. This ambiguity causes the stabilization energies of the N-terminal and C-terminal complexes to be more comparable. In contrast, Ni^{2+} strongly prefers N ligands and a square-planar geometry. Consequently, the stabilization energy of the N-terminal complexes is significantly greater than that of the C-terminal complexes.

Pro as the second to fourth amino acid from the N-terminus inhibits formation of N-terminal square-planar complexes in the gas and solution phases. The only available complexation route for Co^{2+} and Ni^{2+} is formation of unfavorable tricoordinate complexes with the C-terminal carboxylate. The complexes, however, decompose to give more thermodynamically stable square-planar, N-ligand $(y_3 + Cat^{2+} - 2H)^+$ ions, which are directly analogous to aqueous-phase complexes between tripeptides and Ni^{2+}. Weakly abundant C-terminal, distorted square-planar, $(y_4 + Cat^{2+} - 2H)^+$ products arise from even less favored precursors. These more unusual species are detected because the relative stabilization energies of the N and O mixed-ligand precursor complexes are more comparable. The $(y_4 + Cat^{2+} - 2H)^+$ product complexes are directly analogous to solution-phase complexes between Ni^{2+} and Cu^{2+} and tetrapeptides that contain Pro in the first to third positions from the N-terminus.

The fast atom bombardment (FAB) process causes the differences between the solution- and gas-phase chemistry of Co^{2+} and Ni^{2+}. Differences primarily occur in cases in which mass spectrometry detects unfavorable complexes that are undetected in aqueous-phase studies. The FAB process provides energy that can shift the complex equilibria toward formation of less thermodynamically stable species. These species are never highly abundant because they have low densities of states. Their decompositions occur, however, at energies above the threshold. Another difference may occur in cases in which unusual tricoordinate product ions, such as those shown in Scheme 2, are observed. Co^{2+} has a propensity for forming octahedral complexes.[20] Consequently, its octahedral coordination sphere could be filled either by three molecules of water or by matrix ligands from the bombardment solution. In the desolvation process that accompanies gas-phase ion formation, the solvent ligands would be stripped from the precursor complex to leave a tricoordinate, bare peptide complex.

Much aqueous-phase and theoretical chemistry of Ca^{2+} is also reflected in the gas-phase results. Ca^{2+} strongly prefers binding to the C-terminal carboxylate. It does not bind to the N-terminal amine. It also forms flexible complexes of no specific geometry. The solution-phase Ca^{2+} specificity of the -DVP- sequence in staphylococcal nuclease occurs in the gas phase.[16c]

Some gas-phase Ca^{2+} complexes, however, do not form in solution. Ca^{2+} binds neither to deprotonated amides nor to deprotonated side chains of His, Tyr, or other protic peptides,[16] except Asp and Glu, in the aqueous phase. In solution, the pH must be high to deprotonate amides and most protic amino acid side chains to allow subsequent complex formation. At high pH, however, aqueous-phase equilibria overwhelmingly favor precipitation of Ca^{2+} as its hydroxide. Even if a small amount of the complexes is formed, solution-phase techniques would not detect them. In contrast, mass spectrometry detects these unusual deprotonated complexes from their decompositions.

Conclusions

Results for tetrapeptides and larger peptides presented here reveal that the intrinsic (gas-phase) and aqueous-phase chemistries of Ca^{2+}, Co^{2+}, and Ni^{2+} are fundamentally the same. Decompositions of tripeptide complexes do not reveal the intrinsically favored binding interactions. The major differences for Ca^{2+} result from acid–base equilibria that the solvent imposes on the system. Solution-phase binding interactions between Co^{2+} and Ni^{2+} and peptides, however, are intrinsic features of the metal ion and the peptide structures, independent of solvation. This study shows that metastable ion mass spectrometry has a significant potential in directly elucidating important metal ion binding sites in peptides and proteins, a method that before now has been unsubstantiated. We will soon present results from a detailed study of Co^{2+} and Ni^{2+} binding interactions with His and other important peptide side chains. Our future research is in the use of electrospray and tandem mass spectrometry to elucidate metal ion binding sites in larger peptides and proteins.

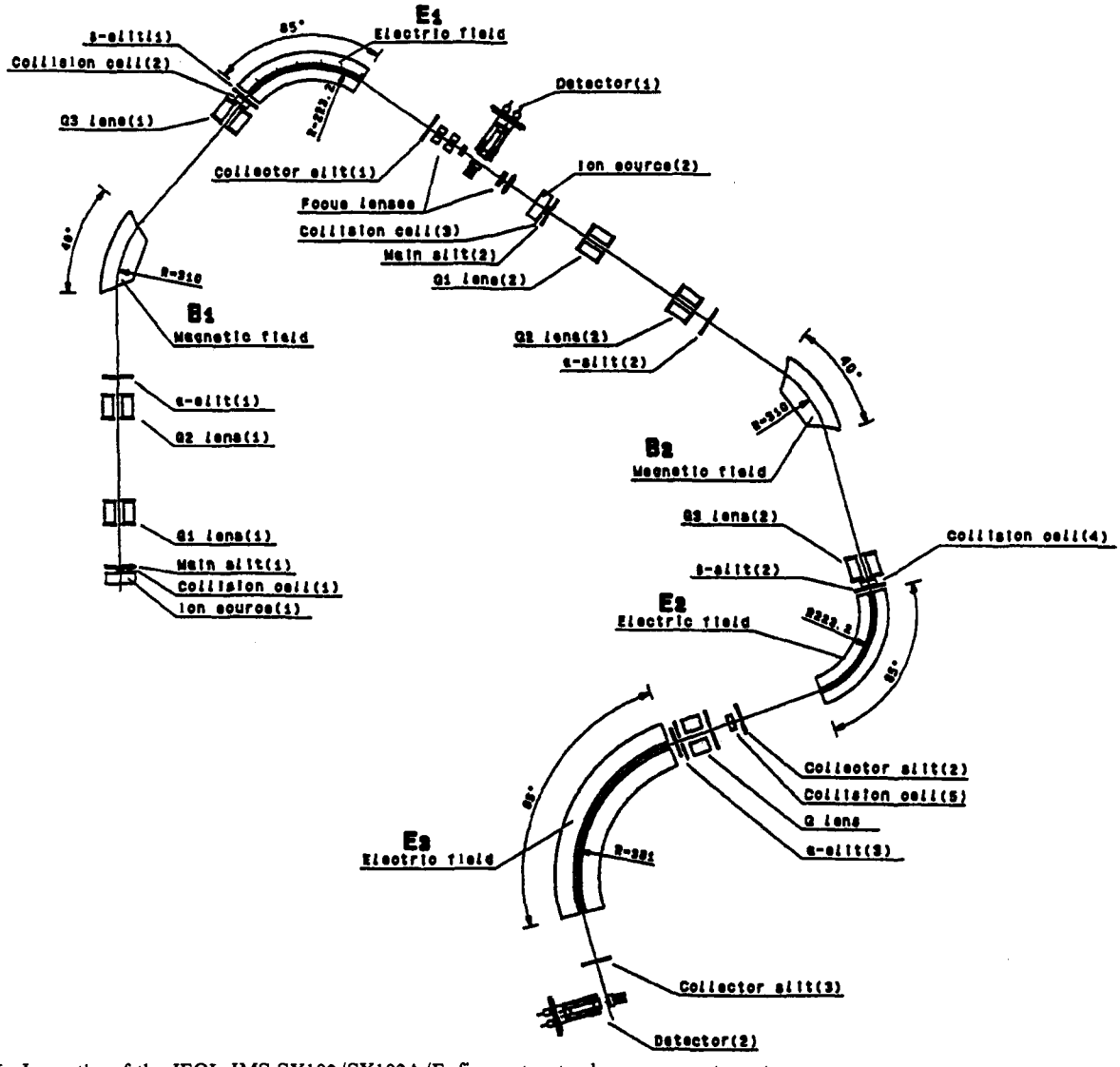

Figure 6. Ion optics of the JEOL JMS-SX102/SX102A/E, five-sector, tandem mass spectrometer.

Experimental Section

Peptides either were purchased from Sigma or Research Plus or were custom synthesized by the Emory University Microchemical Facility. They include ALA, FFF, ALAL, AGFL, GGFM, FFFF, PFGK, VAAF, GGFM, FFGLM-NH_2, FFFFF, GAAAA, VHLGP, YPFAG, GGYFM, GYGFM, YGGFL, YGGFH, HLGLAR, LHGLAR, LGHLAR, SGAGAG, AAAPAA, AADVPA, ADVPAA, SGAGAG, VGVAPG, DTHAAA, ADTHAA, DRVYIHPF, Sar-RVYIHPF, RVYVHPF, and DRVYIHPFHL. The matrix used for fast atom bombardment (FAB) was a 2:1 mixture of thioglycerol/glycerol (T/G) saturated with either $Ca(OH)_2$, $Co(NO_3)_2$, or $Ni(NO_3)_2$. A small amount of the peptide (μg) was mixed with approximately 1 μL of the matrix on a stainless steel FAB probe tip. Deuterium exchange experiments were performed by dissolving the matrix in an equal volume of D_2O. The D_2O was then removed under vacuum. This procedure was repeated three times. The peptides used in these experiments were dissolved in D_2O and allowed to stand at room temperature overnight. To enhance full deuterium labeling, some of the peptides were added to the deuterated matrix and heated for several minutes prior to analysis.

Mass spectrometric experiments were performed by using a JEOL JMS-SX102/SX102A/E, five-sector, tandem mass spectrometer (Figure 6). It is a reverse-geometry instrument of $B_1E_1/B_2E_2/E_3$ configuration (B = magnetic and E = electrostatic analyzer) in which MS1 is B_1E_1, MS2 is B_2E_2, and MS3 is E_3. Precursor ions were produced by bombarding the sample with 3-keV Xe atoms at a gun emission current of 5 mA and were then accelerated to 10 keV. Product ions from MS–MS (MS^2) experiments that were formed in the third field-free region between MS1 and MS2 were observed by scanning MS2 linked to MS3 at a constant ratio of B/E. Precursor and product ion resolution was approximately 1000, and magnet calibration of MS2 was performed by using a mixture of glycerol and CsI. MS–MS–MS (MS^3) experiments were performed by using MS1 to mass- and energy-select the metastable first-generation product ions that were formed in the first field-free region between the ion source and B_1. Their metastable decompositions that occurred in the third field-free region were observed by scanning MS2 linked to MS3 at a constant ratio of B/E.

The semiempirical calculations were performed using a 486-DX66 PC and the program ZINDO[22] as part of the HyperChem software package (Autodesk, Inc.). The program is designed for transition metals, and the parameters were used as provided.

Acknowledgment. We acknowledge the National Science Foundation (CHE-9113272) for funding and the NIH (1S10RR06276) and NSF (CHE-9119862) for the use of the JEOL JMS-SX102/SX102A/E as a shared instrument. We also acknowledge the Emory University Microchemical Facility for the preparation of some of the peptides. Preliminary reports of these results were presented at the 40th and 41th ASMS Conferences on Mass Spectrometry and Allied Topics, May 1992 and 1993, respectively.